Reevaluating the Cr Evaporation Characteristics of Ce/Co Coatings for Interconnect Applications

Citation for the original published paper (version of record):

Reddy, M., Svensson, J., Froitzheim, J. (2021). Reevaluating the Cr Evaporation Characteristics of Ce/Co Coatings for Interconnect Applications. ECS Transactions, 103(1): 1899-1905.
http://dx.doi.org/10.1149/10301.1899ecst

ECS Transactions

The Electrochemical Society
Advancing solid state & electrochemical science & technology

Reevaluating the Cr Evaporation Characteristics of Ce/Co Coatings for Interconnect Applications

To cite this article: Mareddy Jayanth Reddy *et al* 2021 *ECS Trans.* **103** 1899

ECS Transactions, 103 (1) 1899-1905 (2021)
10.1149/10301.1899ecst ©The Electrochemical Society

Reevaluating the Cr Evaporation Characteristics of Ce/Co Coatings for Interconnect Applications

M. J. Reddy[a], J. E. Svensson[a], and J. Froitzheim[a]

[a] Energy and Materials, Chalmers University of Technology Kemivägen 10, 41296
Gothenburg, Sweden

Cathode poisoning by chromium evaporation from the interconnects is one of the major degradation mechanisms in SOFC. Coatings have proved to be very effective in suppressing chromium evaporation on interconnects. The quantification of chromium evaporation is important for determining the chromium consumption in the interconnect and predicting the lifetime of the interconnect. Chromium evaporation of uncoated and Ce/Co coated Crofer 22 APU is reevaluated at 800 °C. The chromium evaporation of Ce/Co coatings on steel sheets and precut steels is studied. Coupons cut from Ce/Co coated sheets have uncoated edges, which influence the chromium evaporation measurements. The true chromium evaporation of the coated interconnects is evaluated. The PVD Ce/Co coatings on Crofer 22 APU reduce the chromium evaporation by at least 60 times compared to the uncoated at 800 °C.

Introduction

Solid oxide fuel cells (SOFC) are high temperature electrochemical devices that convert chemical energy into electrical energy without combustion. They are considered a promising technology for future energy needs. Nevertheless, the commercialization of SOFC is impeded by expensive component materials and high degradation rates. Interconnects are used to stack and electrically connect the individual cells (anode, cathode, and electrolyte) to deliver high power output. A reduction in SOFC operating temperatures has enabled the use of metallic interconnects. Chromia forming ferritic stainless steels (FSS) are extensively researched for their application in interconnects owing to their moderately conducting chromia scale, similar thermal expansion coefficient to the stack components, low cost, and ease of manufacturing. Nevertheless, using chromia forming FSS has some major drawbacks: 1. Chromia scale growth 2. Chromium evaporation. Chromia scale growth leads to increased electrical resistance across the cell. The chromia scale reacts with the air and H_2O to form volatile chromium species Cr (IV). Volatile chromium species react with the cathode and get deposited at the triple-phase boundaries, blocking the oxygen reduction reaction known as cathode poisoning (1). Moreover, the chromium evaporation leads to Cr depletion in the steel, resulting in a less protective scale over time.

Chromium evaporation can be decreased by applying thin-film coatings. The most studied in literature are MCO (Manganese Cobalt Oxide $(Mn,Co)_3O_4$) based coatings applied using various techniques. The combination of reactive element (RE) coatings with MCO coatings was developed to reduce the chromia scale growth. Canovic et al. (2)

showed the beneficial effect of RE addition to cobalt coatings which reduced the chromia scale growth significantly. The quantification of chromia scale growth is usually done by measuring the change of the mass over time, Area Specific Resistance (ASR) measurements, and microscopy; chromium evaporation is measured using the denuder technique (3) and transpiration test (4). Chromium evaporation is much difficult to quantify and is dependent on several factors such as water vapor, flow rate, and the sample orientation to the flow. Thus, similar coatings in the literature have been reported to lower the chromium evaporation of the coated steels by a factor of 2 (5), 10 (6–8), and 50 (9) compared to the uncoated. Chromium evaporation from the same coated material might affect the different stack manufacturers differently based on the humidity, cathode materials, and operating temperature. However, it is important to quantify Cr evaporation to understand the effectiveness of the coatings.

MCO coatings can be applied using the physical vapor deposition (PVD) technique by depositing metallic Co, which upon oxidation becomes Co_3O_4 and is enriched by Mn from the steel substrate during stack operation to form $(Co,Mn)_3O_4$ (2). Applying metallic coatings using a PVD technique can be performed in a large-scale roll-to-roll coating process. The 10 nm Ce + 600 nm Co (Ce/Co) coating has been extensively studied for chromium evaporation, mass gains, and ASR up to 38000 hours (6–8, 10, 11). These studies showed that chromium evaporation on Ce/Co coated steels is decreased by a factor of 10 compared to the uncoated. Nevertheless, the coated samples used for the chromium evaporation measurements are cut from a bigger coated sheet, resulting in uncoated edges. However, the area of edges contributed to only 2-4% of the total surface area of the samples, and this contribution was considered negligible. Hence, the Ce/Co coating is more effective in suppressing chromium evaporation than reported earlier. Therefore, we measured the true chromium evaporation of the coated samples and quantified the chromium evaporation from the uncoated edges of the coated samples.

Experimental Methods

Chromia forming ferritic stainless steel, Crofer 22 APU with a thickness of 0.3 mm, is selected for this study. The composition of the steels is shown in Table 1. Ce/Co coating with 10 nm Ce and 600 nm Co was deposited on the steels using a proprietary Physical Vapor Deposition (PVD) at Sandvik Materials Technology (SMT). The coatings were deposited on a steel sheet, and precut steel sheet, shown in Figure 1.

Table I: Chemical composition of the selected alloy is weight %.

	Fe	Cr	C	Mn	Si	Cu	Ti
Crofer 22 APU	Bal	22.92	0.004	0.38	0.01	0.01	0.06

The experiments were performed at 800 ºC in a tubular furnace in an air atmosphere containing 3% H_2O with a flow rate of 6000 S. min^{-1}. Three coupons of 17 mm x 15 mm x 0.3 mm were used for each exposure in the reactor. The coated coupons cut from coated steel sheet (Fig 1a.) have coated faces and uncoated edges, from now on called sheet-coated. This type of samples have been used in previous research (6, 8, 10–13). The same coating was applied on a pre-cut steel sheet, as displayed in Fig 1b. In this geometry, 17 mm x 15 mm x 0.3 mm are etched out of a steel sheet. The samples are only attached to the sheet by two 1 mm wide sections of the remaining material. Although PVD is a line-of-sight process, some coating material has been deposited on the edges. The coated coupons from the precut steel have thus coated faces and coated edges, from now on called precut-coated. One edge and four edges of the precut-coated coupons were ground to P1200 to remove the coating and are referred to as precut-coated with one ground edge and precut-coated with four ground edges, respectively.

Two types of exposures, mass gain and chromium evaporation, were performed. The time-resolved chromium evaporation behavior of the coupons was investigated using the denuder technique, allowing in-situ determination of chromium evaporation. A detailed description of the measurement procedure is found elsewhere (3). Chromium evaporation exposures were performed on uncoated, sheet-coated, precut-coated, precut-coated with one ground edge, and precut-coated with four ground edges.

The cross-sections of the coated and uncoated samples after the exposure were prepared using Leica EM TIC 3X Broad Ion Beam (BIB). The cross-sections were analyzed using a JEOL JSM-7800F Prime SEM equipped with an Oxford Instruments Energy Dispersive X-ray spectrometer (EDS).

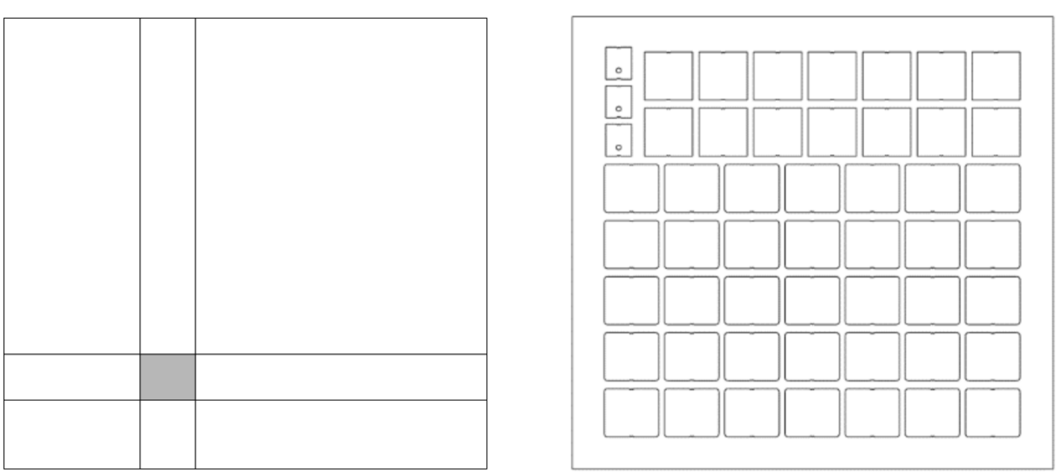

Figure 1: a) Ce/Co coated steel sheet (Grey area represents one coupon with dimensions (17 mm x 15 mm x 0.3 mm)) (b) Ce/Co coated precut steel sheet with varying coupon dimensions.

Results and Discussion

Chromium Evaporation

Figures 2a and 2b show the cumulative chromium evaporation and rate of chromium evaporation of uncoated, sheet-coated Crofer 22 APU exposed at 800 °C for 500 hours. The cumulative chromium evaporation of uncoated and Ce/Co sheet-coated Crofer 22 APU after 500 hours is about 0,093 mg/cm^2 and 0,01 mg/cm^2, respectively. The chromium evaporation on the uncoated coupons is about 10 times higher than Ce/Co sheet-coated coupons. Similar behavior is shown by Ce/Co sheet-coated coupons on different substrates such as Sanergy HT at 650 ºC (8) and 750 ºC (8), AISI 441 at 800 °C (10), 850 °C (6). The rate of chromium evaporation on the uncoated and sheet-coated samples decreased rapidly during the first week and is almost constant for the rest of the exposure. The chromium evaporation reported for sheet-coated coupons has the contribution from both the coated faces and the uncoated edges. Thus, the coatings are more effective in reducing chromium evaporation than depicted by sheet-coated coupons.

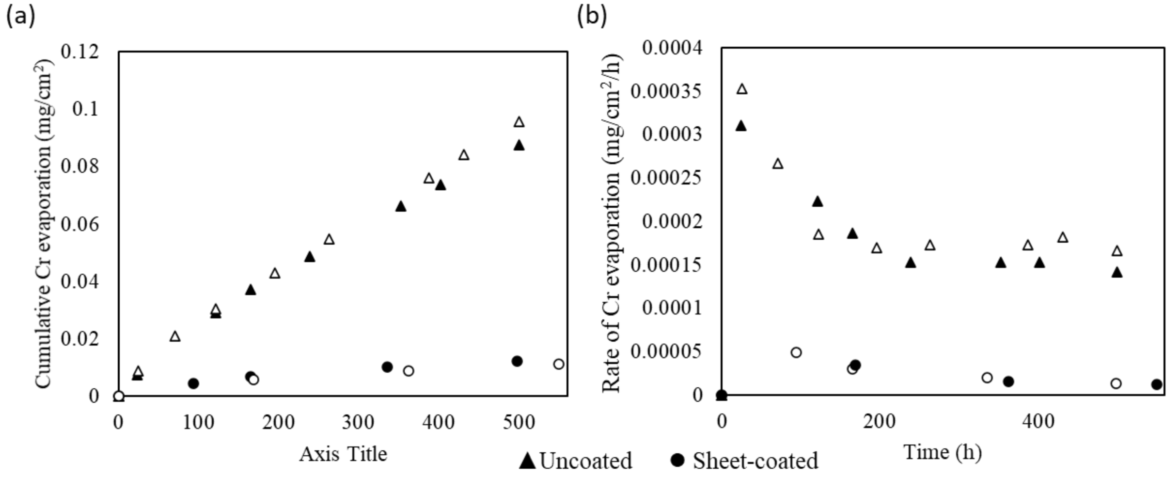

Figure 2: (a) Cumulative chromium evaporation and (b) Rate of chromium evaporation of as a function of time of uncoated (triangles) and sheet-coated (circles) coupons exposed for 500 hours at 800 ºC in air with 3% H_2O. Filled and empty symbols represent two independent exposures.

To better understand the contribution of the uncoated edges in chromium evaporation measurements and the effectiveness of the Ce/Co coating, precut-coated with one ground edge, precut-coated with four ground edges and precut-coated coupons are investigated for chromium evaporation. Figure 3a and 3b show the cumulative chromium evaporation and rate of chromium evaporation of sheet coated, precut-coated with ground edge, precut-coated with four ground edges and precut-coated Crofer 22 APU exposed at 800 °C for 500 hours. The cumulative chromium evaporation of precut-coated with one ground edge and precut-coated Crofer 22 APU after 500 hours is 0,0045 mg/cm^2 and 0,0015 mg/cm^2, respectively. The chromium evaporation of precut-coated coupons is extremely low, almost at the detection limit of the measurement. The chromium evaporation of sheet coated and precut-coated with four ground edges is similar. These results clearly indicate that uncoated edges have a significant contribution to the chromium evaporation on the sheet-coated coupons.

The precut-coated coupons with one ground edge have only 1.2% of the total area as uncoated. Nevertheless, the cumulative chromium evaporation after 500 hours is three times higher than precut-coated coupons. Similarly, sheet-coated coupons have about 4% of the total area as uncoated, but the cumulative chromium evaporation after 500 hours is 6 – 7 times higher than precut-coated coupons. This indicates that the uncoated edges contribute significantly more to the chromium evaporation than estimated from the faces of the uncoated coupons. It is speculated that the flow dynamics inside the reactor lead to higher chromium evaporation along the edges. Further studies are planned to understand this behavior better. However, the higher chromium evaporation on the edges might not affect the chromium evaporation measurements on the uncoated coupons since the edges contribute only 4% of the total uncoated area.

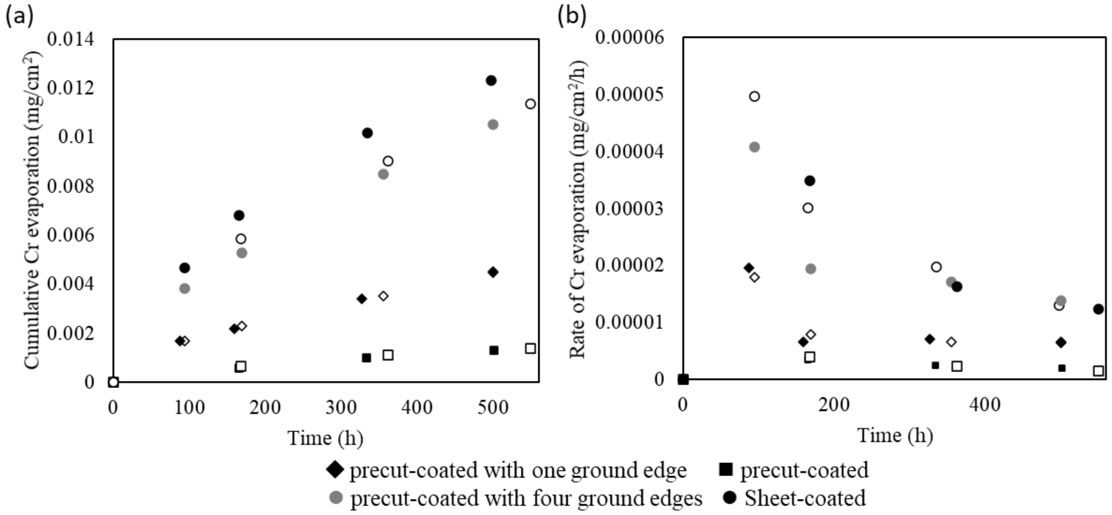

Figure 3: (a) Cumulative chromium evaporation and (b) Rate of chromium evaporation of as a function of time of sheet-coated (black circles), precut-coated with four ground edges (grey circles), precut-coated with one ground edge (rhombus), and precut-coated (squares) coupons exposed for 500 hours at 800 ºC in air with 3% H_2O. Filled and empty symbols represent two independent exposures.

Oxidation Kinetics:

Figures 4a and b show the net mass gain and gross mass gains of the coated and uncoated Crofer 22 APU exposed at 800 °C for 500 hours. The net mass gain plotted in figure 4a is the combination of mass gain due to oxidation and mass loss due to chromium evaporation. To understand the true extent of the oxidation and Cr consumption in the alloy, one needs to compensate for net mass gain with material lost due to chromium evaporation. The gross mass gain in figure 4b represents the total oxidation which is the sum of net mass gain and chromia evaporated (extrapolated from figure 2b).

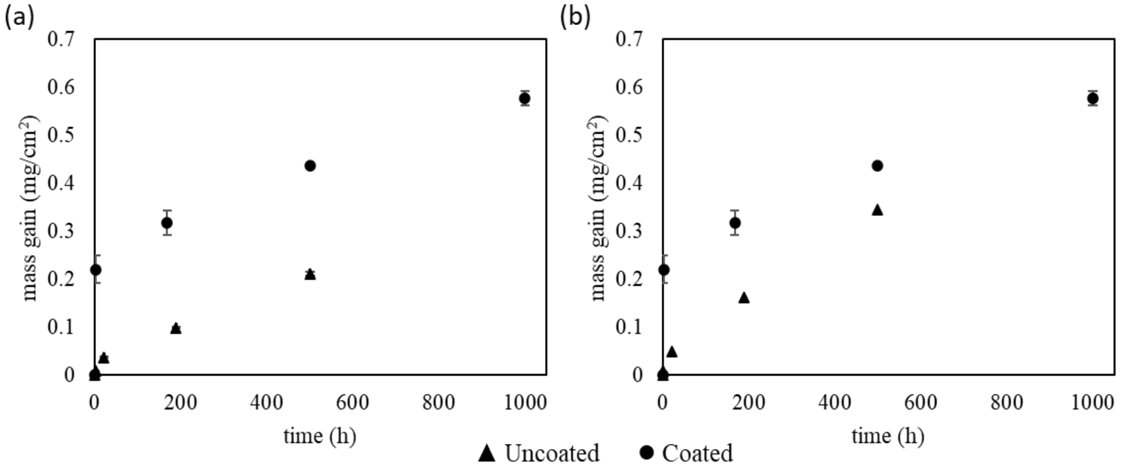

Figure 4: (a) Net mass gain and (b) gross mass gain of uncoated and Ce/Co coated Crofer 22 APU exposed at 800 °C in air with 3% H_2O for 500 h and 1000h, respectively.

The gross mass gain is much higher than the net mass gain for the uncoated due to high chromium evaporation. No significant difference between the net mass gain and gross mass gain is observed for the coated coupons due to much lower chromium evaporation. Moreover, the sheet-coated and precut-coated coupons showed no major differences in the net or gross mass gains. The application of Ce/Co coating significantly reduced the Cr consumption in the alloy.

Microstructural analysis:

Figure 5a and b shows the SEM micrographs and corresponding EDX maps of uncoated and Ce/Co coated coupons exposed at 800 °C for 500 hours and 1000 hours, respectively. Uncoated coupons show a two-layered structure with $(Cr,Mn)_3O_4$ on the top and Cr_2O_3 beneath it. The coated coupons show a similar two-layered structure but with $(Co,Mn)_3O_4$ doped with Fe on the top and Cr_2O_3 scale beneath it. $(Co,Mn)_3O_4$ is very effective in reducing chromium evaporation.

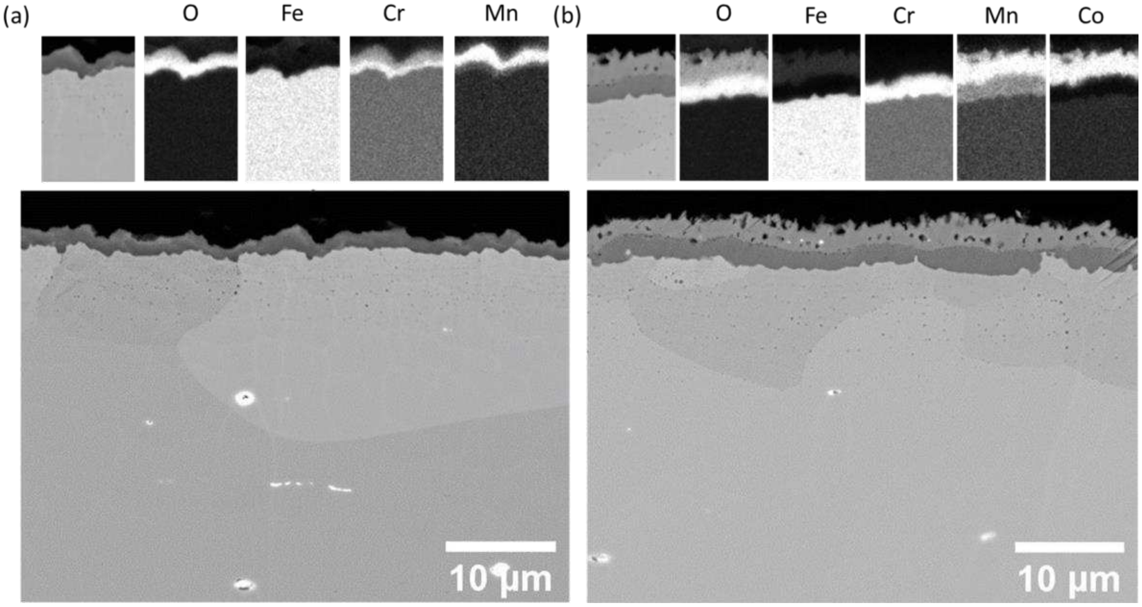

Figure 5: SEM micrographs and corresponding EDX maps of (a) uncoated and (b)Ce/Co coated coupons exposed at 800 °C for 500 hours and 1000 hours, respectively.

Conclusions

Ce/Co coating on Crofer 22 APU is investigated for chromium evaporation and oxide scale growth at 800 °C. The coated samples showed lower oxide scale growth and chromium evaporation than the uncoated ones. A significant difference in the chromium evaporation between the uncoated, coated coupons with uncoated edges, coated coupons with coated edges is observed. The coated coupons with coated edges have much lower chromium evaporation, about 60 times lower than the uncoated at 800 °C. Overall, the PVD coated Ce/Co coatings are more effective in suppressing chromium evaporation than earlier reported.

Acknowledgments

This work was performed within the Swedish High Temperature Corrosion Centre. This project has received funding from the Fuel Cells and Hydrogen 2 Joint Undertaking under Grant Agreement No 826323. This Joint Undertaking receives support from the European Union's Horizon 2020 Research and Innovation programme, Hydrogen Europe and Hydrogen Europe Research.

References

1. S. P. Jiang, and X. Chen, *Int. J. Hydrogen Energy*, **39**, 505 (2014).
2. S. Canovic, J. Froitzheim, R. Sachitanand, M. Nikumaa, M. Halvarsson, L. G. Johansson, and J. E. Svensson, *Surf. Coatings Technol.*, **215**, 62 (2013).
3. J. Froitzheim, H. Ravash, E. Larsson, L. G. Johansson, and J. E. Svensson, *J. Electrochem. Soc.*, **157**, B1295 (2010).
4. A. N. Aphale, B. Hu, M. Reisert, A. Pandey, and P. Singh, *JOM*, **71**, 116 (2019).
5. T. Thublaor, and S. Chandra-ambhorn, *Corros. Sci.*, **174**, 108802 (2020).
6. J. G. Grolig, J. Froitzheim, and J. E. Svensson, *J. Power Sources*, **248**, 1007 (2014).
7. C. Goebel, R. Berger, M. W. Lundberg, J. Westlinder, J.-E. Svensson, and J. Froitzheim, *ECS Trans.*, **78**, 1675 (2017).
8. H. Falk-Windisch, J. Claquesin, M. Sattari, J. E. Svensson, and J. Froitzheim, *J. Power Sources*, **343**, 1 (2017).
9. B. Talic, H. Falk-Windisch, V. Venkatachalam, P. V. Hendriksen, K. Wiik, and H. L. Lein, *J. Power Sources*, **354**, 57 (2017).
10. C. Goebel, R. Berger, C. Bernuy-Lopez, J. Westlinder, J. E. Svensson, and J. Froitzheim, *J. Power Sources*, **449**, 227480 (2020).
11. H. Falk-Windisch, M. Sattari, J. E. Svensson, and J. Froitzheim, *J. Power Sources*, **297**, 217 (2015).
12. J. Froitzheim, S. Canovic, M. Nikumaa, R. Sachitanand, L. G. Johansson, and J. E. Svensson, *J. Power Sources*, **220**, 217 (2012).
13. M. Tomas, C. Goebel, J.-E. Svensson, and J. Froitzheim, *ECS Trans.*, **91** (1), 2291 (2019).